JOURNAL OF AIRCRAFT
Vol. 40, No. 4, July–August 2003

Stiffness Scaling for Solid-Cloth Parachutes

H. Johari* and K. J. Desabrais†
Worcester Polytechnic Institute, Worcester, Massachusetts 01609

The parameters affecting the inflation of solid-cloth, flat circular parachute canopies were investigated. A primary dimensionless parameter in addition to mass ratio, Froude number, and permeability is a stiffness index. Comparison of sub- and full-scale C9 parachutes, along with small-scale wind- and water-tunnel models has revealed that a relative stiffness index is able to correlate the filling and opening times of various sized canopies. The filling and opening times can be expressed as the relative stiffness index raised to power -0.064, with a proportionality factor of 1.3 for the filling time. The proportionality factor that correlates opening times is 0.86 for mass ratios in the range of 0.1–0.2, and it approaches 1.3 as mass ratio becomes very large. The index has utility in correlating peak forces as well.

Nomenclature

a	=	sound speed
C_F	=	force coefficient, $F/q\ S_o$
C_F^*	=	peak force coefficient
c	=	characteristic velocity through fabric (permeability)
c_d	=	suspension line drag coefficient
$D_{\max}$	=	maximum canopy width when hung upside down
D_o	=	canopy constructed diameter
D_p	=	mean projected canopy diameter
d_s	=	suspension line damping factor
E	=	fabric modulus of elasticity
F	=	fluid force on the canopy
F_l	=	force on the payload
Fr	=	Froude number, V_s/gD_o
F^*	=	peak force on the canopy
F_l^*	=	peak force on the payload
g	=	gravitational constant
I	=	canopy second moment of area
k_s	=	suspension line spring constant
l_s	=	suspension line length
M	=	Mach number, V_s/a
MR	=	payload mass ratio, $m_l/\rho D_o^3$
MR_c	=	canopy mass ratio, $m_c/\rho D_o^3$
m_c	=	canopy mass
m_l	=	payload mass
n	=	number of suspension lines
q	=	dynamic pressure, $\frac{1}{2}\rho V_s^2$
$\bar{q}$	=	dynamic pressure averaged over canopy inlet area
Re	=	Reynolds number, $\rho V_s D_o/\mu$
r	=	local radius of curvature
S_o	=	constructed canopy area, $\pi D_o^2/4$
t	=	time
t_f	=	filling time
$t_{\max}$	=	time at maximum diameter
t_o	=	opening time
V_s	=	snatch velocity
V_∞	=	constant freestream velocity
W	=	canopy weight
w	=	fabric areal density
α	=	angle of attack
Δp	=	pressure differential across canopy fabric
δ	=	canopy fabric thickness
δ_s	=	suspension line diameter
ζ	=	relative stiffness index, $\{E/[\rho V_s^2(1-\nu^2)]\}(\delta/D_o)^3$
η	=	stiffness index, $(D_{\max}/D_o)(W/wS_o)$
μ	=	fluid viscosity
ν	=	fabric Poisson's ratio
ρ	=	fluid density
τ	=	normalized time, tV_s/D_o
τ_f	=	normalized filling time, $t_f V_s/D_o$
τ_o	=	normalized opening time, $t_o V_s/D_o$

Introduction

FROM a parachute designer's point of view, the three most significant performance parameters besides parachute stability are the peak opening force, opening (or filling) time, and the drag during steady descent, that is, steady-state drag. These parameters are typically obtained from full-scale testing of parachute prototypes. Full-scale testing for design purposes is time consuming and not cost effective. A better understanding of the flowfield surrounding the parachute canopy may help significantly with the preliminary design of new parachute systems and even address questions regarding stability. Assessment of the flowfield in the immediate vicinity (including the near wake) of a full-scale parachute canopy is quite difficult, unless the parachute is tested in a wind tunnel or simulated using sophisticated computational fluid–structure interaction (FSI) algorithms.[1,2] However, at the present time, only a few parachute systems can be simulated accurately. Owing to the large deformations of the canopy during inflation and the necessary computational mesh movement, the inflation phase appears to be beyond the capability of the FSI computations at the present time. On the other hand, wind (or water) tunnels provide a controlled environment for measuring the flow in the wake of parachute canopies. Except for very large-scale wind tunnels, blockage limitations typically require the canopy to be scaled down. Cockrell[3] states that a blockage ratio of $\sim 5\%$ or less is required to faithfully reproduce the flowfield around a parachute canopy in a wind tunnel.

Scaling of parachute performance parameters has been pursued by several investigators, both for round and parawing-type canopies. Fu,[4] Lingard,[5] and Heinrich and Hektner,[6] among others, have performed dimensional analysis to correlate parachute parameters such as the opening force and opening time. Because the findings of Fu relate to the subsequent discussions, a brief description of his model is presented here. In the model, the canopy and the payload are considered as two point masses connected by a spring. Based on this assumption, and through employment of the conservation of mass, Newton's second law, and geometric constraints, a set of differential equations is derived. The opening/filling times and forces

Presented as Paper 2001-2007 at the AIAA 16th Aerodynamic Decelerator Systems Technology Conference, 21–24 May 2001; received 31 January 2002; revision received 2 October 2002; accepted for publication 12 February 2003.

*Professor, Mechanical Engineering Department. Associate Fellow AIAA.
†Graduate Student, Mechanical Engineering Department; currently Research Aerospace Engineer, U.S. Army, Natick Soldier Center, Airdrop Technology Team, Natick, MA 01760. Member AIAA.

are calculated by the model. The canopy geometry is prescribed *a priori* during the inflation phase. In the model, all of the aerodynamic forces are lumped into inputted drag coefficients for the canopy and the payload.

Although many studies in the past have attempted to relate full-scale performance parameters of different parachute systems, few studies have considered the scaling down of one type of parachute canopy. For example, Lingard[5] measured the opening forces on a 40-cm, solid-cloth, flat circular canopy in air and water under finite and infinite mass conditions. More recently, Lee[7] has compared the opening time and peak opening force of free-falling one-quarter, one-half, and full-scale C9 parachutes. Although he found that the smallest (one-quarter scale) canopy generally had the highest normalized peak opening force and the smallest normalized opening time, no concrete relationship was found to correlate the full-scale and subscale results. Changes in the canopy stiffness and permeability (mean flow velocity through the fabric) were thought to be responsible for the observed variations in the measured opening parameters. Furthermore, Lee suggested that lighter fabrics be used in the construction of subscale models. A difficulty with this suggestion is that lighter fabrics generally have different permeability and strength characteristics.

Niemi[8,9] analyzed the available literature on the scaling of parachute canopies, paying particular attention to stiffness. He derived a relative stiffness index, based on the earlier work of Kaplun[10] and Knacke,[11] that also contained dynamic parameters such as the snatch velocity. It appears that the relative stiffness index of Niemi correlated reasonably well with the normalized opening times of Lee's[7] C9 parachutes. It turned out that a power law relationship exists between the normalized opening time and the relative stiffness index of Niemi. In contrast, the peak opening force did not appear to correlate with this relative stiffness index.

Thus far, it appears that Niemi's relative stiffness index has only been used to correlate finite mass inflations. The 3-ft (91-cm) canopy of Heinrich and Noreen[12] and the 80-cm canopy of Lingard[5] in a wind tunnel (plus a 40-cm canopy in a water tank) appear to be the smallest-scale solid-cloth, flat circular canopies that have been inflated under controlled conditions. Heinrich and Noreen measured the projected area of the canopy during the inflation, as well as during the force time history. From these measurements, Heinrich[13] concluded that the projected diameter time history during finite and infinite mass deployments have minimal differences. Lingard measured the projected diameter and drag of inflating small-scale canopies under finite and infinite mass conditions. The small scale of the canopies chosen in his studies was dictated by the need to keep the blockage ratio to a minimum.

We are investigating the flowfield in the near wake of flat circular canopies in a low-speed water tunnel during inflation and steady-state (terminal descent) phases.[14,15] We are employing 15- and 30-cm solid-cloth canopies in a 60-cm square cross section water tunnel. The blockage ratios for these $\frac{1}{56}$th and $\frac{1}{28}$th scale C9 models during steady state are approximately 2.5 and 10%, respectively. Note that, during inflation, the blockage is even less. The low-speed water tunnel was chosen because it produces longer opening times than a wind tunnel at comparable Reynolds numbers with the same scale model, and the particle image velocimetry technique was implemented in the water tunnel with relative ease. This technique allows the measurement of the velocity field in a plane at a sufficient spatial resolution to enable the calculation of the vorticity field in the near wake of the canopy. The velocity field measurements are presented elsewhere.

In this paper, a detailed dimensional analysis of parameters that are relevant solely to the aerodynamics of an inflating parachute canopy, as well as those that are relevant to the performance of the entire parachute system, are presented first. Note that the majority of past studies have only considered the entire system and not necessarily the specific issues related to the canopy aerodynamics. The relative importance of matching various parameters is enumerated. Following the dimensional analysis, a comparison of the parameters for full- and small-scale solid-cloth, flat circular canopies in air and water is presented, along with an expression for the correlation of the filling and opening times with a stiffness index applicable to the very small-scale models and full-scale parachutes.

Dimensional Analysis

The parameters affecting the aerodynamics of the parachute canopy are considered first in the analysis to be presented, and then the entire parachute system, including the effects of suspension lines and payload, is examined. As far as the canopy aerodynamics is concerned, the primary independent parameters to be considered are the fluid force exerted on the canopy and the mean projected canopy diameter. From the time history of these two parameters, the peak force F^*, the opening time t_o (the time from the instant the lines become taut to the time of peak opening force), and the filling time t_f (the time when the projected canopy diameter first reaches the mean steady-state diameter) can be found. Other independent parameters are ρ, μ, and a, as well as V_s (or the constant freestream velocity V_∞ in infinite mass cases), α (with respect to the symmetry axis), m_c, D_o, δ, an equivalent fabric modulus of elasticity E, and ν. The Poisson's ratio relates the lateral strain to the longitudinal strain in the fabric. Because nylon fabrics used in the construction of parachute canopies possess a complex stress-strain relationship, data from uniaxial tests performed on nylon fabrics in the warp and fill directions were utilized.[8,9] The mean Young's modulus in the warp and fill directions were averaged and used as the equivalent modulus of elasticity. The numerical values of the equivalent modulus of elasticity and Possion's ratio were taken from Refs. 8 and 9.

Nylon fabrics used in parachute canopies are permeable, meaning that the imposition of a pressure differential across the fabric results in a net flow through the fabric. Permeability is characterized by a mean velocity c across the canopy fabric; this velocity depends on the fabric pore size and the pressure differential across the fabric. Although these latter parameters may be included in the dimensional analysis, the inclusion of the integral measure c at the appropriate pressure differential suffices. It is also important to distinguish between porosity, which denotes the geometric porosity (fabric area divided by the constructed area) of the canopy due to the cut pattern, and permeability. The porosity is dictated by the canopy design, whereas the permeability is a fabric property and not a design parameter.

Accounting for the preceding parameters in a dimensional analysis results in the following relationships.

$$
\begin{aligned}
C_F \equiv F/qS_o &= f_1\left(\tau, Re, M, \alpha, c/V_s, \delta/D_o, m_c \Big/ \rho D_o^3, E/q, \nu\right)\\
D_p/D_o &= f_2\left(\tau, Re, M, \alpha, c/V_s, \delta/D_o, m_c \Big/ \rho D_o^3, E/q, \nu\right)\\
\tau_o \equiv t_o V_s/D_o &= f_3\left(Re, M, \alpha, c/V_s, \delta/D_o, m_c \Big/ \rho D_o^3, E/q, \nu\right)\\
\tau_f \equiv t_f V_s/D_o &= f_4\left(Re, M, \alpha, c/V_s, \delta/D_o, m_c \Big/ \rho D_o^3, E/q, \nu\right) \quad (1)
\end{aligned}
$$

If the flow profile upstream of the canopy is not uniform, then another parameter q/q, characterizing the ratio of the average (over the canopy area) dynamic pressure to the assumed dynamic pressure has to be added to the preceding parameters.

Other canopy properties, such as the mean fabric strain, can also be written as a function of the preceding parameters. If the strain is expressed as the tension in the fabric ($r \cdot \Delta p$) over ($\delta \cdot E$), then the strain is proportional to $(q/E)(D_o\delta)$. These terms are clearly present in the preceding set of parameters, justifying the exclusion of fabric strain from Eq. (1).

Although stiffness of the canopy is not directly present in the preceding set of parameters, it is a function of the last four dimensionless parameters in the arguments of Eq. (1), that is, the canopy thickness ratio δD_o, the canopy mass ratio MR_c, normalized modulus of elasticity E/q, and fabric Poisson's ratio. Alternatively, the stiffness index η proposed by Heinrich and Hektner[6] and defined as $\eta = (D_{\max}/D_o)(W/w\,S_o)$ can be replaced in Eq. (1). Lee[7] reports that a standard C9 has an η of 0.15, with $D_{\max} = 0.077\,D_o$. However, note that η appears to be applicable only to canopies made from the same fabric and with similar construction.

If the entire parachute system, including the suspension lines and the payload, is considered in the analysis, the following parameters need to be brought in: m_l, g, as well as the suspension line parameters l_s, δ_s, k_s, d_s, n, and c_d. Once these parameters are nondimensionalized, the force experienced by the payload will have a form as follows:

$$C_F \equiv F_l/qS_o = f(\tau, Re, M, \alpha, \mathrm{MR}_c, \delta/D_o, c/V_s, E/q, \nu, Fr,$$
$$\mathrm{MR}, l_s/D_o, \delta_s/D_o, k_s/qD_o, d_s/\rho V_s S_o, n, c_d) \quad (2)$$

In addition to geometric similarity, all of the preceding dimensionless parameters have to be similar between a model and full-scale parachute to achieve complete similarity. Because it is not possible to match all of these parameters between full- and subscale canopies, the relative significance of each parameter has to be considered.

Reynolds number Re, which denotes the ratio of inertia to viscous forces, is on the order of 10^6–10^7 for full-scale parachute canopies. It is believed that the Reynolds number does not play a crucial role during the inflation and terminal descent of round canopies.[5] Cockrell[3] provides data on the steady-state drag coefficient of full-scale canopies at lower speeds that indicate a dependence on Reynolds number. These variations are thought to stem from the variation of the mean projected diameter with Reynolds number. Once the drag is normalized with the projected area (as opposed to the constructed area), the Reynolds number effect should be minimal. As long as the flow separates at the lip of a canopy (and $Re > 10^4$), no Reynolds number effect is expected.

M is an indicator of the compressibility effects. Macha[16] reports that Mach number effects appear gradually for $0.4 < M < 0.9$. For the low-speed applications and small-scale models tested in low-speed tunnels, Mach number has little effect on the parachute performance parameters.

The initial α of the parachute canopy is determined from the flight trajectory, and is an important parameter in determination of the drag if it changes significantly during the inflation phase. For round canopy models held in a wind tunnel, small changes in α do not have an appreciable effect on the opening time and drag coefficient.

Permeability of the canopy fabric, as characterized by c/V_s, is an important similarity parameter because it affects the flow in the near wake of the canopy. Permeability of the canopy fabric is thought to affect large-scale vortical motions behind bluff bodies. Increase of drag coefficient and decrease of opening time is expected with a reduction in permeability. Permeability appears to be even more important under infinite mass conditions. Wolf[17] presents data from flight- and wind-tunnel tests that reveal that geometric porosity is a dominant factor in the peak opening force of parachutes at infinite mass conditions.

MR_c is an indicator of the inertia of the canopy fabric and has been recognized in the past by Kaplun[10] and Niemi[8,9] as an important factor. During infinite mass inflations, the canopy mass ratio is a dominant factor because the overall mass ratio becomes immaterial. The canopy mass ratio is also a factor in Niemi's relative stiffness index ζ. For full-scale canopies, the canopy mass ratio is typically less than 0.01, which indicates that the inflation rate is minimally affected by inertia of the canopy. Thus, for subscale testing, care should be exercised so that the canopy mass ratio is kept as small as possible.

MR, characterizes the ratio of the payload mass to the air mass included in the canopy. The latter is approximately represented by ρD_o^3. The payload mass ratio is a primary factor in the determination of the peak opening force of finite mass parachute systems. For sub-scale testing purposes, this parameter has to be equal to that of the full-scale system. Theoretical models of Fu[4] and Lingard[18] have both shown that the peak opening force increases at first with increasing payload mass ratio and then decreases.

Froude number Fr has long been recognized as a principal parameter governing the peak opening load of parachute systems. Theoretical models and experimental data suggest that the shock factor (the peak opening force over the payload weight) is a linear function of Froude number.[18] Of course, for infinite mass inflations in a wind tunnel, Froude number does not play a role.

The dimensionless parameters associated with suspension lines are l_s/D_o, δ_s/D_o, $k_s/(qD_o)$, $d_s/(\rho V_s S_o)$, n, and c_d. The first two parameters, along with the number of suspension lines n, are purely geometrical parameters and could be duplicated in subscale models. The cable drag coefficient is a function of the Reynolds number of the cable and can be a nonnegligible portion of the total fluid dynamic drag at slow speeds. The remaining two parameters are the effective parachute spring and damping constants. If the damping term is re-written as $n d_s D_o/m_l V_s$, Fu[4] has shown that this damping-related parameter has a minimal effect on the canopy inflation rate. The effective parachute spring constant can also be written as $nk_s D_o^2/m_l V_s^2$, which is also expected to have a minimal effect on the parachute performance parameters, as long the latter has a value greater than two.[4]

The remaining two parameters E/q and ν are the canopy fabric parameters that contribute to the stiffness of the canopy. As mentioned earlier, E, ν, and δ can be replaced with the empirical stiffness index of Heinrich and Hektner.[6] However, we suggest that the relative stiffness index of Niemi be used in place of η because the former is a dynamic parameter containing the snatch velocity and the drop altitude (through density). Moreover, Niemi's index combines several of the other dimensionless parameters, thus reducing the total number of parameters. The relative stiffness as first proposed by Kaplun[10] has the following form $EI/(qD_o^4)$. Utilizing plate deflection theory, Niemi[8] writes the relative stiffness index as

$$\zeta = \left\{E \Big/ \left[\rho V_s^2 (1 - \nu^2)\right]\right\}^{(\delta/D_o)^3}$$

which can be applied to both finite and infinite mass inflations. This index can be rewritten as

$$\{[E/(1 - \nu^2)w](\delta/D_o)^3\}(\mathrm{MR}_c/Fr)$$

if the snatch velocity is rewritten in terms of the Froude number. The terms in the braces are only a function of the canopy fabric and scale, whereas the ratio in the last set of parentheses depends on the drop conditions.

Based on the preceding discussion, the time history of the force on the payload in low-speed applications becomes a function of the following parameters:

$$C_F \equiv F_l/qS_o = f(\tau, Fr, \mathrm{MR}, \zeta, \alpha, c/V_s, l_s/D_o, k_s/qD_o) \quad (3)$$

Therefore, a subscale parachute model is expected to reproduce the force time history accurately if the Froude number, payload mass ratio, relative stiffness index, angle of attack, fabric permeability, fineness ratio, and the parachute spring constant are matched between the sub- and full-scale systems. The peak opening force and opening (or filling) time can similarly be written as

$$C_F^* \equiv F_l^* \Big/ qS_o = f(Fr, \mathrm{MR}, \zeta, \alpha, c/V_s, l_s/D_o, k_s/qD_o)$$
$$\tau_o \equiv t_o V_s/D_o = f(Fr, \mathrm{MR}, \zeta, \alpha, c/V_s, l_s/D_o, k_s/qD_o) \quad (4)$$

Data from Berndt and De Weese[19] for full-scale C9 parachute tests suggest that the filling time τ_f is only a function of the mass ratio, and τ_f becomes nearly constant for MR greater than ~ 0.1. Fu's model[4] also shows the predicted filling time to be very nearly independent of the Froude number and spring constant. Moreover, for standard rip-stop nylon at typical airdrop snatch velocities, the permeability is quite small, of the order of a few percent. Of course, if the permeability (or geometric porosity) increases, we expect the filling time to increase as well. Thus, for the range of parameters in routine airdrop applications, it is expected that the filling (or opening) time be a function of the relative stiffness index ζ, the initial angle of attack α, and only a weak function of MR, except at very low mass ratios. Data from Lee's[7] 1989 vertical drop tests of one-quarter, one-half, and full-scale C9s at a mass ratio of 0.13 can be fitted reasonably well with a power law dependence on the relative stiffness index.[8,9] The expression for the opening time was $\tau_o = 0.86\zeta^{-0.064}$. We will examine this power law dependence on ζ

for our very small-scale (relatively stiff) canopies. It is expected that the proportionality factor is a function of the canopy geometry and permeability. Filling time is also expected to have a similar form, but with a different factor.

Concerning the peak opening force, Lingard[18] states that the load factor, that is, $F_l^*/m_l g$, is a linear function of the Froude number. When the load factor is rewritten in terms of the normalized peak opening force multiplied by (Fr/MR) it reveals that C_F^* is only a function of the mass ratio, relative stiffness index, and permeability. Lingard's semi-empirical theory for canopy inflation further assumes that C_F is a unique function of time and mass ratio. Note that Lee's load factor data for a one-quarter scale C9 appear to follow a weaker than linear dependence on Froude number.

For our small-scale canopy models, which inflate horizontally in a water tunnel under infinite mass conditions, the peak opening force should only depend on the relative stiffness index and the suspension line spring constant. The permeability of standard nylon fabrics in water is quite small and effectively equivalent to the impermeable F111 fabric. The filling time is expected to depend on the relative stiffness index alone. In the next section, various dimensionless parameters are compared among full- and subscale C9 canopies inflating in air and water.

Experimental Data

Five different solid-cloth, flat circular parachute canopies are considered here. They are a full-scale C9, Heinrich's 3-ft (91-cm) wind-tunnel model,[13] our 12-in. (30-cm) water tunnel model, and our 6-in. (15-cm) model tested in a wind and water tunnel. The very small scale of the models considered in this study required that special construction techniques be employed so that the stiffness could be reduced as much as possible. The canopies were made from one solid piece of standard 1.1 oz/yd^2 rip-stop nylon fabric, instead of individual gores being sewn together (see Fig. 1). They were manufactured by cutting the material around a flat circular template at the appropriate diameter. The edge of the nylon material was seared, to prevent it from fraying. All of the models had a fineness ratio of unity ($l_s = D_o$) and 24 suspension lines. The suspension lines, which were 100-μm nylon thread, were attached to the canopy by a small loop being tied at the end of the suspension line that was passed through a hole near the edge of the canopy skirt. The suspension lines were attached to a stationary streamlined forebody in the tunnel, as shown in Fig. 2. The forebody diameter was about 9% of the smallest model canopy diameter, which resulted in minimal interference with the inflation. The model canopies were inflated under constant freestream velocity, mimicking infinite mass conditions.

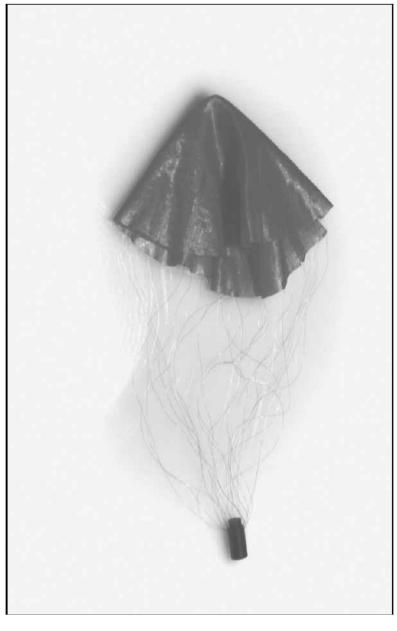

Fig. 1 Parachute canopy model, 15 cm (6-in.).

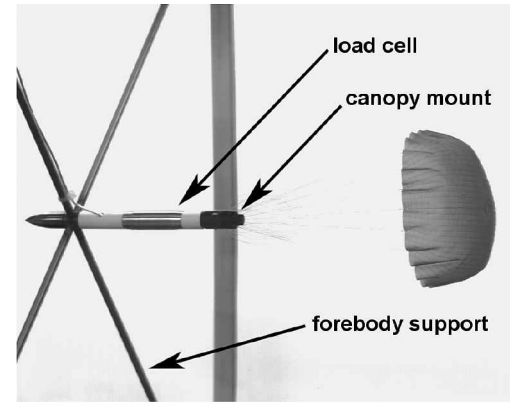

Fig. 2 Forebody support arrangement in the water tunnel.

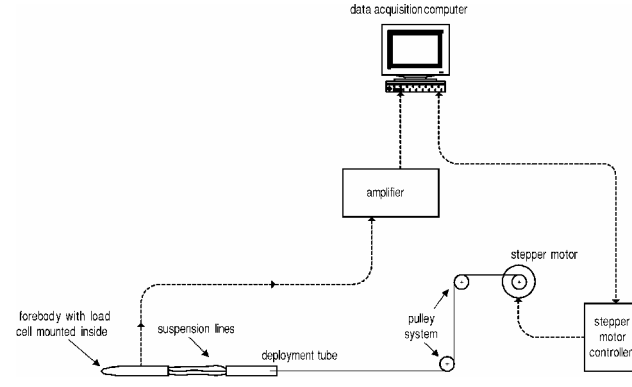

Fig. 3 Schematic of the deployment tube and the setup in the water tunnel.

The canopies were packed into a round deployment tube downstream of the forebody, which was pulled away to start the inflation process. The inner diameter of the deployment tube was 0.07 D_o. The deployment tube was pulled away by a thin nylon string that passed through a series of pulleys and was attached to a stepper motor. The stepper motor extracted the deployment tube at a time that was synchronized with the force measurement and the imaging systems. A schematic of the setup is shown in Fig. 3. The details of the canopy construction and the experimental setup can be found in Refs. 20 and 21.

The drag was measured by a load cell located inside the forebody and attached directly to the suspension lines. The load cell output was sampled at 150 Hz with a 12-bit A/D card. The canopy was imaged by a high-resolution progressive-scan charge-coupled device camera at a 30-Hz framing rate. The images were analyzed by an automated image processing program that computed the maximum projected canopy diameter to within 1%.

The inflation of the 15-cm model at a constant freestream velocity of 0.2 m/s in the water tunnel is shown in a sequence of images in Fig. 4. Initially, the canopy was packed into the deployment tube and the canopy was positioned such that the suspension lines were taut. At time $t = 0.0$ s, the deployment tube was pulled away (Fig. 4a). Once the deployment tube had cleared the canopy, it initially took on a cylindrical shape (Fig. 4b), which then transitioned into a conical shape (Fig. 4c). Over this period, the canopy diameter had grown to one-half of its fully inflated diameter. The fluid then proceeded to fill the canopy from the skirt toward the top of the canopy, creating a nearly hemispherical canopy shape (Fig. 4d). With the upper region of the canopy filled, the inflation of the canopy proceeded toward the skirt until the canopy diameter reached its steady-state diameter (Fig. 4e). The maximum force the canopy experiences occurred after the canopy had become hemispherical in shape, but before it achieved its maximum diameter. The canopy then overexpanded beyond its steady-state diameter, achieving its maximum diameter in Fig. 4f. After the maximum projected diameter was achieved, the

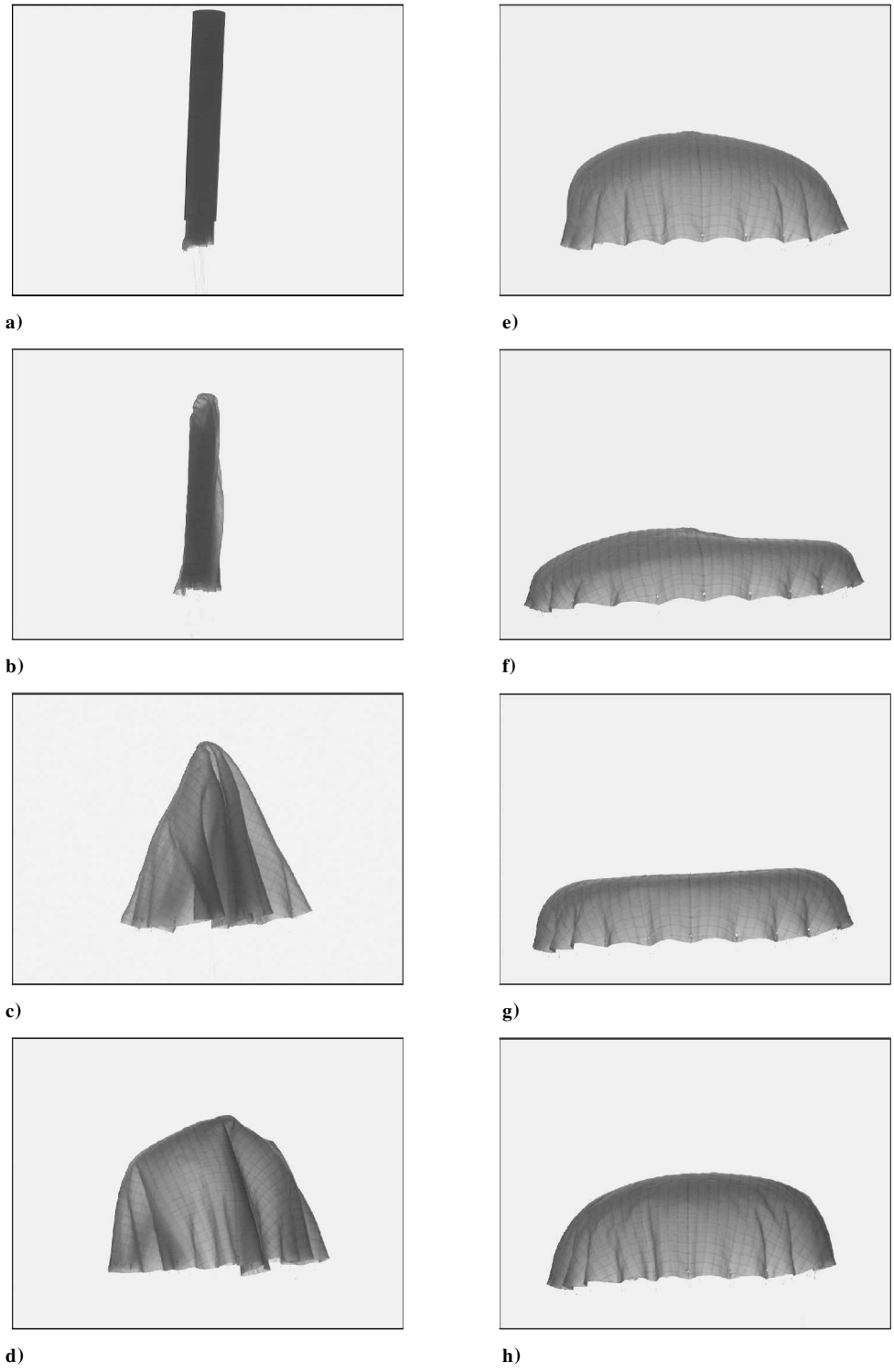

Fig. 4 Sequence of images showing the inflation of the 15-cm (6-in.) model in the water tunnel at a constant freestream velocity of 0.2 m/s: a) $t = 0.00$ s, b) $t = 0.23$ s, c) $t = 1.00$ s, d) $t = 1.23$ s, e) $t = 1.43$ s, f) $t = 1.70$ s, g) $t = 2.00$ s, and h) $t = 2.27$ s.

canopy diameter shrank and the canopy geometry began to approach that seen under steady descent. During the inflation process, the canopy inflated nearly symmetrically and remained centered on axis. Only after the canopy had reached the overexpanded state did the canopy wander off axis. The geometry of the 30-cm model canopy during the inflation was similar to that of the 15-cm model.

Two characteristics of the small-scale model canopies that differ from larger and full-scale canopies should be noted. First, the initial conical shape of the small-scale canopies is different from that of full-scale canopies, which typically form a more cylindrical shape during the early stage of inflation. At these small scales, the material stiffness becomes more apparent.[6] For a given fabric, larger canopies are more flexible. Second, the maximum diameter of the small-scale models typically occurred at the canopy skirt throughout the entire inflation process, whereas for full-scale canopies, the maximum diameter is not necessarily at the canopy skirt. During the inflation, full-scale canopies inflate from the apex toward the skirt, and the maximum diameter occurs at a point between the apex and the skirt.

Table 1 Dimensionless inflation characteristics of small-scale water-tunnel models

D_o, m (in.)	V_s, m/s	τ_f	τ_o	C_F^*
0.30 (12)	0.20	1.91 ± 0.40	1.94 ± 0.44	3.61 ± 0.42
0.15 (6)	0.39	2.07 ± 0.38	2.18 ± 0.44	2.91 ± 0.69
0.15 (6)	0.20	2.10 ± 0.50	2.07 ± 0.58	3.48 ± 0.80

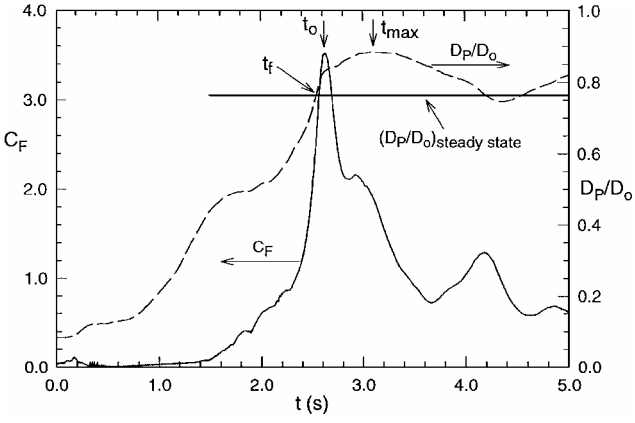

Fig. 5 Time traces of force coefficient and projected diameter for the 30-cm (12-in.) model inflated under the infinite mass condition, velocity is 0.2 m/s.

Again, the stiffness of the small-scale models affects the flexibility of the canopy.

A typical force and maximum projected diameter trace for the 30-cm model inflated in the water tunnel at a speed of 0.2 m/s is shown in Fig. 5. As expected, the drag rises slowly at first while the canopy is unfolding. The projected diameter has an inflection point at approximately $0.5D_o$, beyond which both the projected diameter and drag increase rapidly. The force coefficient reaches its maximum value of 3.5 at a time of 2.63 s and then drops rapidly. There are several large-amplitude oscillations in the drag force before it settles into its steady-state value. The maximum projected diameter reaches a maximum value of $0.88D_o$ during the over-inflated phase, before settling into its steady-state breathing mode with an average diameter of $0.76D_o$. The horizontal solid line in Fig. 5 shows the mean diameter during steady state. The point at which the diameter curve crosses the solid line is the filling time, as indicated in Fig. 5. The opening and maximum diameter times are also shown in Fig. 5. Table 1 lists the average measured filling and opening times, along with the maximum force coefficient for the 15- and 30-cm models inflated in the water tunnel at constant velocity. The standard deviations of the normalized parameters are also included in Table 1 and are approximately 20% of the average values. The relatively large standard deviations are a result of the unsystematic unfolding of the canopy and not the uncertainty of the measurements. The measurement uncertainties are approximately 1% and are significantly smaller than the standard deviations of the data. Such large standard deviations are also present in full-scale tests. For our small-scale models, the filling time is generally within 5% of the opening time. This is consistent with the commonly accepted notion that infinite mass inflations result in the opening time being the same as the filling time.[11] The maximum force coefficients in our experiments are also consistent with those measured by Lingard[5] for similarly scaled water-tunnel models.

Major dimensionless parameters of Reynolds number, permeability, thickness ratio, canopy mass ratio, and the two stiffness indices are listed in Table 2 for full- and small-scale C9s. The velocity for the two water-tunnel models was chosen to produce the same Reynolds number of 6.7×10^4; the wind-tunnel model had a velocity that resulted in a Reynolds number comparable to that of the water-tunnel models. The last column in Table 2 shows the range of payload mass ratio used in the finite mass experiments. The same canopy fabric was used in all of the canopies listed in Table 2; therefore, the fabric material properties are all the same. They are: $E = 4.69 \times 10^8$ Pa, $\nu = 0.14$, $w = 0.032$ kg/m^2 (0.94 oz/yd^2), and $\delta = 7.1 \times 10^{-5}$ m (0.0028 in.). Note that, because E, ν, and δ are all the same among the different canopy sizes compared in Table 2, the variation in ζ is due solely to variations in the fluid density, snatch velocity, and canopy diameter. The implications of this on the proposed correlations will be discussed in the next section.

Because our small-scale canopies were made of a solid piece of fabric, the Heinrich and Hektner[6] stiffness index becomes $\eta \cong D_{\max}/D_o$. Measurement of $D_{\max}$ for our models revealed that η was 0.5 and 0.43 for the 6- and 12-in. models, respectively. These values are to be compared against a value of 0.15 for the full-scale C9 as reported by Lee[7] and 0.6 for the Heinrich 3-ft model. The large η value for the latter is due to the full-scale construction methods employed on that model.

The permeability for the different canopy sizes in Table 2 was calculated based on the standard air permeability at 0.5-in. water pressure differential. The permeability of the water models is based on the measurements reported by Lingard.[5]

There are several interesting observations with regard to the dimensionless numbers in Table 2. The permeability parameter is comparable among all cases considered, except for the smallest 6-in. air model that has a value approximately three times higher than the others. The canopy mass ratio is smallest for the two water-tunnel models, even smaller than that associated with the full-scale canopy. This is due to the large density difference between air and water. Thus, the inertia of the canopy itself is negligible in the water-tunnel models, as is the case for the full scale. On the other hand, the 3-ft and 6-in. air models have substantially larger canopy mass ratios. The relative stiffness index increases as the velocity and canopy diameter decrease, as expected. The range for ζ covers nearly eight orders of magnitude among the cases considered. Even with such a large range for ζ, the stiffness index η of Heinrich varies over a relatively narrow range. This is because both the snatch velocity and canopy diameter are present in the relative stiffness index ζ.

The column designated by D_o/V_s in Table 2 has dimensions of time and is included to provide a timescale for the inflation process. The largest timescale of 1.5 s belongs to the 12-in. water-tunnel model; the smallest timescale of 25 ms belongs to the 6-in. wind-tunnel model. The rest have time scales of the order of a few tenths of a second. These data reveal the extreme frequency response required of the instrumentation used for testing small-scale canopies in a wind tunnel. Relatively long inflation times can be had in water at reasonable Reynolds numbers.

Correlation of Data

Because the opening time varies with mass ratio, our measured infinite mass opening times can not be correlated with the widely available opening times for mass ratios in the 0.1–0.2 range. For low mass ratios, the opening time is smaller than the filling time, whereas the two times are comparable for high mass ratio inflations. Therefore, filling time was chosen as the parameter to be correlated for small models and the full-scale C9.

The filling times of full-scale C9 as reported by Berndt and DeWeese,[19] the 3-ft model of Heinrich and Noreen,[12] along with our small-scale models, are plotted in Fig. 6 against the relative stiffness index ζ. The best-fit power law to the data is $1.3\zeta^{-0.064}$, which indicates the efficacy of this index in correlating filling times for different scale canopies over the large range of ζ. The exponent of -0.064 in this expression is the same as that found by Niemi when correlating Lee's[7] opening times of one-quarter, one-half, and full-scale C9s at a mass ratio of 0.13. However, there are no filling time data available for one-half or one-quarter scale C9s. Note that even though the small-scale models had different geometries during the inflation than the full-scale C9s, their filling time still correlates well with the larger and full-scale canopies. This further demonstrates the versatility of the relative stiffness index in accounting for the variations in canopy stiffness.

Based on the preceding correlation, we suggest that the power-law first proposed by Niemi[8,9] is a valuable tool for scaling the filling and opening time of solid-cloth, flat circular canopies. The

Table 2 Dimensionless parameters for C9 parachutes with different scales

Canopy C9	Re	c/V_s	δ/D_o	MR_c	ζ	η	D_o/V_s, s	MR
28 ft (air)	$\sim 10^7$	<0.02	8.3×10^{-6}	5.4×10^{-3}	10^{-11} _ 10^{-9}	0.15	0.1–0.5	0.15–0.4
3 ft (air)	1.3×10^6	0.017	7.8×10^{-5}	0.08	4.0×10^{-7}	0.6	0.4	0.24
12 in. (water)	6.7×10^4	0.012	2.3×10^{-4}	1.1×10^{-4}	1.5×10^{-4}	0.43	1.5	∞
6 in. (water)	6.7×10^4	0.021	4.7×10^{-4}	2.1×10^{-4}	3.1×10^{-4}	0.5	0.4	∞
6 in. (air)	6.3×10^4	0.06	4.7×10^{-4}	0.17	1.1×10^{-3}	0.5	0.025	∞

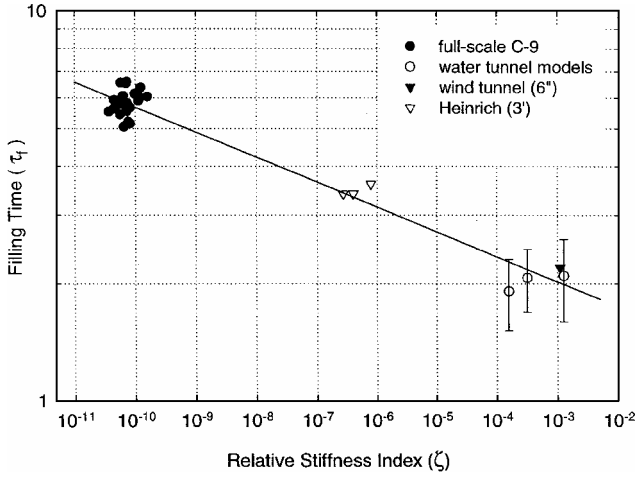

Fig. 6 Dependence of the filling time on the relative stiffness index, —— is the best power law fit to the data.

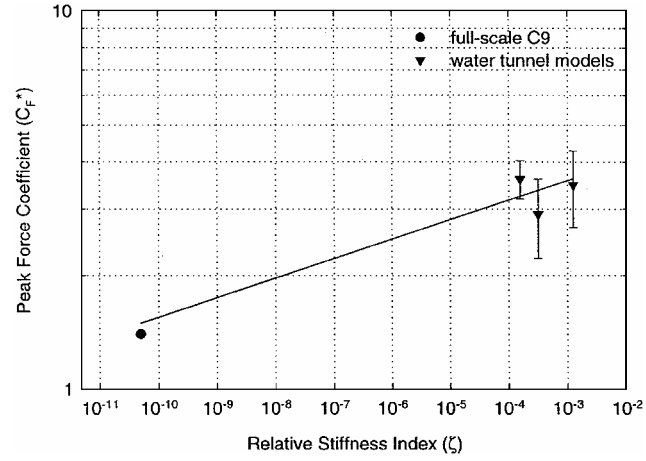

Fig. 7 Peak force coefficient as a function of the relative stiffness index at infinite mass conditions; power law fit to the limited data is shown.

preceding expression is applicable to both infinite and finite mass inflations. It is suggested that the exponent _0.064 is universal for all solid-cloth, flat circular type canopies. On the other hand, the proportionality factor depends on whether the filling or opening time is considered. Furthermore, this factor should be independent of the mass ratio (based on the payload or total mass) as long as the mass ratio is greater than about 0.1. All past studies have indicated a rapid increase of filling time with MR as it gets smaller than $\sim$0.1. The proportionality factor is also expected to depend on the permeability of the fabric, as tested under the pertinent pressure differential across the fabric. As the permeability increases, the proportionality factor should increase. Finally, care should be taken when data from drop tests are considered in the evaluation of the robustness of any correlation because of the variability of the canopy angle of attack at the start of the inflation process.

As stated earlier, the variations in the relative stiffness index in the current experiments stems from the changes in fluid density, velocity, and canopy diameter, and not from the fabric material properties. Thus, the proposed correlation is strictly applicable to flat, circular canopies with the standard 1.1 (0.94 actual) oz/yd^2 fabric. However, the earlier work of Niemi has shown that the relative stiffness index is also capable of correlating the opening time full- and subscale C9 canopies constructed from the different (heavier) fabrics. Based on this evidence, we suggest that the correlation should hold for different canopy fabrics, perhaps with a different proportionality factor.

The peak opening force of a full-scale C9 inflating under infinite mass condition is plotted in Fig. 7 along with our measured peak force coefficients. As expected, C_F^* increases as the canopy becomes stiffer. Unfortunately, there are no data available for the peak forces on subscale C9 parachutes at infinite mass conditions. A power law fit of the form $C_F^* = 5.0\zeta^{.05}$ for the limited data results in a reasonable correlation. Certainly, more data are needed to validate this scaling. Data on the inflation of our small-scale models at finite mass are needed to allow correlation with the full- and subscale data of Lee.[7] For finite mass inflations, the load factor should be correlated with the index ζ for each mass ratio to bypass the effects of Froude number. Niemi[22] has suggested that the peak opening force of finite mass inflations can be correlated through a "modified impulse" parameter that incorporates the relative stiffness parameter. The definition of this parameter and the correlation procedure are described in Ref. 22. However, the resulting correlation between the theory and the data of Lee[7] is only fair.

Conclusions

A detailed dimensional analysis of the parameters affecting the inflation of solid-cloth flat circular canopies was carried out. The canopy aerodynamics in isolation and the entire parachute system were considered separately. Comparison of sub- and full-scale C9 parachutes along with small-scale wind- and water-tunnel models have revealed that a single parameter, namely, the relative stiffness index, is able to correlate the filling and opening times of various canopy sizes. The filling time, normalized by the constructed diameter and snatch velocity, is

$$\tau_f = 1.3\zeta^{-0.064} = 1.3\left(\left\{E \Big/ \left[\rho V_s^2(1 - \nu^2)\right]\right\}\frac{(\delta/D_o)^3}{}\right)^{-0.064} \qquad (5)$$

The opening time for mass ratios in the range of 0.1–0.2 can also be expressed as follows:

$$\tau_o = 0.86\zeta^{-0.064} \qquad (6)$$

The proportionality factor in the last expression depends on the mass ratio and increases by up to 50% as the mass ratio becomes large. Fabrics with large permeability are expected to produce proportionality factors that are different from those in the preceding expressions. The utility of the effective stiffness index in correlating the peak opening force needs to be investigated at the same mass ratio for a range of canopy sizes.

Acknowledgment

This material is based on work supported by the U.S. Army Research Office under Grant DAAG55-98-1-0171.

References

[1] Stein, K. R., "Simulation and Modeling Techniques for Parachute Fluid–Structure Interactions," Ph.D. Dissertation, Dept. of Aerospace Engineering, Univ. of Minnesota, Twin Cities, MN, Dec. 1999.

[2]Stein, K., Benney, R., Kalro, V., Tezduyar, T. E., Leonard, J., and Accorsi, M., "Parachute Fluid–Structure Interactions: 3-D Computation," *Computer Methods in Applied Mechanics and Engineering*, Vol. 190, 2000, pp. 373–386.

[3]Cockrell, D. J., "The Aerodynamics of Parachutes," 295, AGARDograph, AGARD, NATO (ISBN 92-835-0422-4) 1987.

[4]Fu, K.-H., "Theoretical Study of the Filling Process of a Flexible Parachute Payload System," German Air and Space Research and Test Inst., Research Rept. DLR-FB 75-76, Brunswick, Germany, Aug. 1975.

[5]Lingard, J. S., "The Aerodynamics of Parachutes During the Inflation Process," Ph.D. Dissertation, Dept. of Aeronautical Engineering, Univ. of Bristol, Bristol, England, U.K., Oct. 1978.

[6]Heinrich, H. G., and Hektner, T. R., "Flexibility as a Model Parachute Performance Parameter," *Journal of Aircraft*, Vol. 8, No. 5, 1971, pp. 704–709.

[7]Lee, C. K., "Modeling of Parachute Opening: An Experimental Investigation," *Journal of Aircraft*, Vol. 26, No. 5, 1989, pp. 444–451.

[8]Niemi, E. E., Jr., "An Improved Scaling Law for Determining Stiffness of Flat, Circular Canopies," U.S. Army Natick Research, Development, and Engineering Center, TR-92/012, Natick, MA, March 1992.

[9]Niemi, E. E., Jr., "An Improved Canopy Stiffness Scaling Law for Determining Opening Time of Flat Circular Parachutes," *Proceedings of the AIAA 8th Applied Aerodynamics Conference*, AIAA, Washington, DC, 1990, pp. 201–212.

[10]Kaplun, S., "Dimensional Analysis of the Inflation Process of Parachute Canopies," Aeronautical Engineer Thesis, Aeronautics Department, California Inst. of Technology, Pasadena, CA, 1951.

[11]Knacke, T. W., *Parachute Recovery Systems Design Manual*, Para Publishing, Santa Barbara, CA, 1992.

[12]Heinrich, H. G., and Noreen, R. A., "Analysis of Parachute Opening Dynamics with Supporting Wind-Tunnel Experiments," *Journal of Aircraft*, Vol. 7, No. 4, 1970, pp. 341–347.

[13]Heinrich, H. G., "Opening Time of Parachutes Under Infinite Mass Conditions," *Journal of Aircraft*, Vol. 6, No. 3, 1969, pp. 268–272.

[14]Desabrais, K. J., and Johari, H., "Near-Field Wake of a Generic, Round Parachute Canopy in Steady Flow," AIAA Paper 2001-1037, Jan. 2001.

[15]Desabrais, K. J., and Johari, H., "Flowfield in the Near Wake of an Inflating Parachute Canopy," *Proceedings of the 16th AIAA Aerodynamic Decelerator Systems Technology Conference*, AIAA, Reston, VA, 2001, pp. 122–130.

[16]Macha, J. M., "An Introduction to Testing Parachutes in Wind Tunnels," AIAA Paper 91-0858, May 1991.

[17]Wolf, D., "Parachute Opening Shock," *Proceedings of the CEAS/AIAA 15th Aerodynamic Decelerator Systems Technical Conference*, AIAA, Reston, VA, 1999, pp. 253–257.

[18]Lingard, J. S., "A Semi-Empirical Theory to Predict the Load-Time History of an Inflating Parachute," *Proceedings of 8th Aerodynamic Decelerator and Balloon Technology Conference*, AIAA, New York, 1984, pp. 117–185.

[19]Berndt, R. J., and DeWeese, J. H., "Filling Time Prediction Approach for Solid Cloth Type Parachute Canopies," *Proceedings of AIAA Aerodynamic Decelerator Systems Conference*, Houston, TX, Sept. 1966, p. 454.

[20]Desabrais, K. J., and Johari, H., "Reynolds Number and Scale Effects on Inflating Parachute Canopies," *Proceedings of the CEAS/AIAA 15th Aerodynamic Decelerator Systems Technical Conference*, AIAA, Reston, VA, 1999, pp. 258–268.

[21]Desabrais, K. J., "Velocity Field Measurements in the Near Wake of a Parachute Canopy, Ph.D. Dissertation, Mechanical Engineering Dept., Worcester Polytechnic Inst., Worcester, MA, April 2002.

[22]Niemi, E. E., Jr., "Impulse Approach for Determining Parachute Opening Loads for Canopies of Varying Stiffness," *Proceedings of the AIAA 11th Aerodynamic Decelerator Systems Technical Conference*, AIAA, Washington, DC, 1991, pp. 316–322.